8300 *Biochemistry* **2010,** *49,* 8300–8306
DOI: 10.1021/bi100957h

BIOCHEMISTRY
including biophysical chemistry & molecular biology
Article

The *BCL-2* 5′ Untranslated Region Contains an RNA G-Quadruplex-Forming Motif That Modulates Protein Expression[†]

Ramla Shahid,[‡] Anthony Bugaut,*[,‡] and Shankar Balasubramanian*[,‡,§,∥]

[‡]*Department of Chemistry, University of Cambridge, Lensfield Road, Cambridge CB2 1EW, U.K.,* [§]*School of Clinical Medicine, University of Cambridge, Cambridge CB2 0SP, U.K., and* [∥]*Cancer Research UK, Cambridge Research Institute, Li Ka Shing Centre, Cambridge CB2 0RE, U.K.*

Received June 14, 2010; Revised Manuscript Received August 20, 2010

ABSTRACT: The *BCL-2* gene encodes a 25 kDa membrane protein that plays critical roles in the control of apoptosis. The regulation of *BCL-2* gene expression is highly complex and occurs both transcriptionally and posttranscriptionally. In particular, the 5′ upstream region of *BCL-2* contains a number of elements that control its expression. We have identified a highly conserved 25-nucleotide G-rich sequence (BCL2Q), with potential to fold into a RNA G-quadruplex structure, located 42 nucleotides upstream of the translation start site of human *BCL-2*. In this study, we used a series of biophysical experiments to show that the BCL2Q sequence folds into a stable RNA G-quadruplex in vitro, and we conducted functional luciferase reporter-based assays, in a cell-free lysate and in three types of human cell lines, to demonstrate that the BCL2Q sequence modulates protein expression in the context of the 493-nucleotide native 5′ untranslated region of *BCL-2*.

The *BCL-2* gene (B-cell lymphoma gene 2) is a member of the Bcl-2 family of proteins composed of pro- and anti-apoptotic factors that serve as essential points in programmed cell death (*1*). It encodes a 25 kDa membrane protein that functions to prevent apoptosis (*2*). The *BCL-2* gene was first identified by its involvement in t(14;18) chromosomal translocation, which is associated with human follicular lymphomas (*3*−*5*). As a result of the translocation, one allele of the anti-apoptotic *BCL-2* gene from chromosome 18 is juxtaposed to the immunoglobulin heavy-chain locus on chromosome 14. This translocation leads to up-regulated expression of Bcl-2 protein, and high levels of *BCL-2* mRNA[1] are detected in cells with the t(14;18) chromosomal translocation (*5*, *6*). Increased cell survival due to elevated levels of expression of *BCL-2* has been correlated to the development of B-cell lymphomas and confers resistance to a variety of anticancer therapies (*7*, *8*). In addition, deregulated expression of *BCL-2* is not restricted to lymphomas. High levels of Bcl-2 protein and/or aberrant patterns of Bcl-2 protein production have been observed in a variety of solid tumors (*9*−*13*), whereas insufficient expression in neuronal cells has been associated with neurodegenerative diseases, including Alzheimer's and Parkinson's diseases (*14*, *15*).

With such an important role in regulating apoptosis, the expression of *BCL-2* is highly regulated at multiple levels, both transcriptionally and posttranscriptionally. In particular, the 5′ upstream region of the *BCL-2* gene contains a number of elements that control its expression (Figure 1). Two main promoters, P1 and P2, regulate the transcription of *BCL-2*; both promoters contain multiple transcription initiation sites that give rise to transcripts containing 5′ untranslated regions (UTRs) differing in size by ∼1.4 kb (*16*). The regulation of these two promoters is highly complex and depends on both tissue type and developmental stage (*17*, *18*). In many cell types, the vast majority of *BCL-2* transcripts are derived from the P1 promoter, whereas the P2 promoter, which is negatively regulated by the p53 protein, shows no or minimal activity (*16*, *19*). However, usage of the P2 promoter is activated in t(14;18) lymphoma cells (*16*, *19*, *20*). A novel promoter region (M) with a p53-dependent activity, located between P1 and P2, was recently identified that counteracts the suppressive activity of P2 on P1 (*21*). In addition, the 5′ UTR of transcripts initiated from the upstream promoter contains a 221-nucleotide alternatively spliced intron. The splicing frequency of this intron varies among cell lines, although both spliced and unspliced forms are often simultaneously expressed (*16*). Several studies have revealed a lack of correlation between the levels of *BCL-2* mRNA and Bcl-2 protein in various cell lines, indicating that translational and posttranslational control mechanisms also play a significant role in regulating Bcl-2 protein levels (*22*−*24*).

Many posttranscriptional regulatory pathways involve sequence and/or structural elements within the UTRs of mRNAs (*25*). The *BCL-2* 5′ UTR is highly conserved among several species, suggesting a regulatory role for this region (*26*−*28*). Indeed, elements that regulate translation have already been identified within the *BCL-2* 5′ UTR (*29*, *30*). We and others have recently demonstrated that RNA G-quadruplex-forming sequences within the 5′ UTRs of mammalian genes can modulate translation efficiency both in cell-free experiments and in mammalian cell tissue culture (*31*−*38*). G-Quadruplexes are non-canonical four-stranded nucleic acid structures that arise from the stacking of hydrogen-bonded G-tetrads (*39*). Our computational searches for putative RNA G-quadruplex-forming sequences in 5′ UTRs in the human transcriptome have revealed

[†]We thank the BBSRC for project funding and Cancer Research UK for program funding. We thank the Cambridge Commonwealth Trust and the COMSATS Institute of Information Technology for studentship funding (R.S.).

*To whom correspondence should be addressed. A.B.: phone, +44 1223 746686; e-mail, ab605@cam.ac.uk. S.B.: phone, +44 1223 336347; e-mail, sb10031@cam.ac.uk.

[1]Abbreviations: UTR, untranslated region; uORF, upstream open reading frame; IRES, internal ribosome entry site; UV, ultraviolet; CD, circular dichroism; T_m, melting temperature; mRNA, messenger RNA.

 Published on Web 08/20/2010

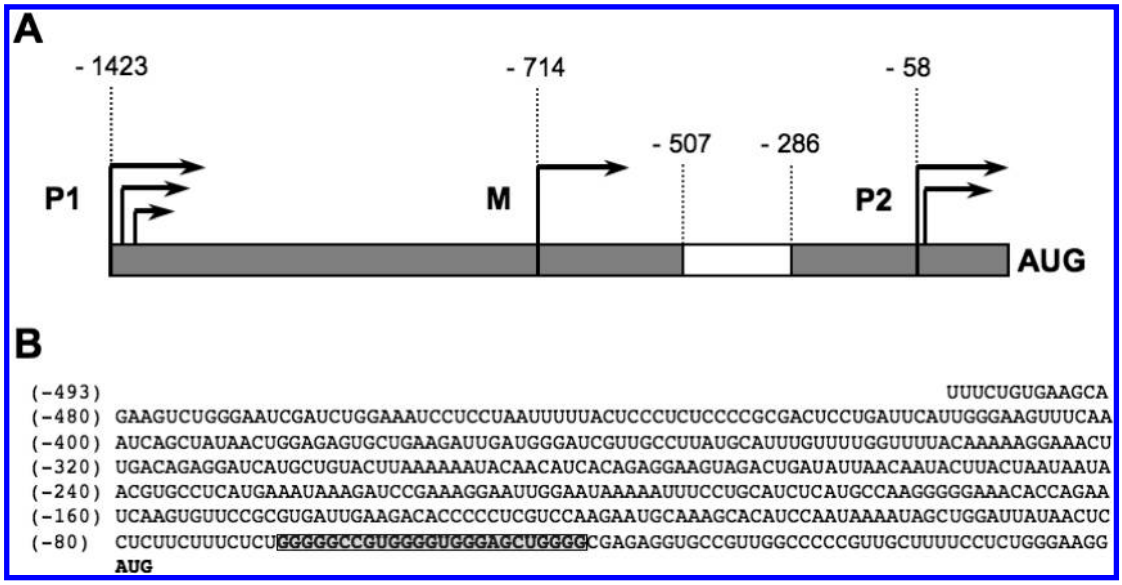

FIGURE 1: (A) Schematic representation of the 5′ upstream region of the *BCL-2* gene. The white section represents an alternatively spliced intron. (B) Sequence of the *BCL-2* 5′ UTR used in this study. The BCL2Q RNA G-quadruplex-forming sequence is boxed.

Table 1: Conservation of the RNA G-Quadruplex-Forming Sequence in the 5′ UTR of *BCL-2*

species	sequence[a]	position[b]
human	**GGGGG**CCGU**GGGGU**GGGAGCU**GGGG**	−42
chimpanzee	**GGGGG**CCGU**GGGGU**GGGAGCU**GGGG**	−42
macaque	**GGGGG**CCGU**GGGGU**GGGAGCU**GGGG**	−42
gorilla	**GGGGG**CCGU**GGGGU**GGGAGCU**GGGG**	−42
orangutan	**GGGGG**CCGU**GGGGU**GGGAGCU**GGGG**	−42
mouse	**GGGGG**CCGU**GGGGC**GGGAGUC**GGGG**	−43
rat	**-GGGG**CCGU**GGGGC**GGGAGCC**GGG-**	−43
dog	**GGGGG**CCGC**GGGGC**GGGAGCA**GGGG**	−43
horse	**GGGGG**CUGU**GGGGC**GGGAGCA**GGGG**	−45
dolphin	**GGGGG**CCGU**GGGGC**GGGAAGC**GGGG**	−44

[a]Sequences were retrieved from Ensembl (release 57). Nucleotides in bold are runs of guanines capable of forming G-quadruplexes. [b]Distance (in nucleotides) between the last G of the putative quadruplex and the translation start site.

the presence of a highly G-rich sequence (BCL2Q, 5′-GGGGGCCGUGGGGUGGGAGCUGGGG-3′), with potential to fold into an RNA G-quadruplex structure, located 42 nucleotides upstream of the translation start site of the human *BCL-2* (*32*, *40*). This motif is highly conserved, in both its sequence and its position relative to the translation start site, across various species (Table 1), suggesting a potentially important biological function for this sequence. Herein, we describe biophysical experiments that demonstrate that the BCL2Q sequence folds into a stable RNA G-quadruplex in vitro and functional luciferase reporter assays, in a cell-free lysate and in human cells, that show that the BCL2Q sequence modulates protein expression in the context of the native 493-nucleotide 5′ UTR of *BCL-2*.

MATERIALS AND METHODS

CD and UV Spectroscopy. Thermal UV melting and CD measurements were performed as previously described (*32*, *35*), using an HPLC-purified synthetic RNA oligonucleotide of the BCL2Q sequence (IBA Gmbh). The UV thermal difference spectrum was obtained as previously described (*41*).

Construction of Plasmids. The 493-nucleotide *BCL-2* 5′ UTR was PCR-amplified from human genomic DNA (Promega) using *Pfu* DNA polymerase. The UTR is present in two exons, 207 nucleotides in exon 1 and 286 nucleotides in exon 2, separated by an alternatively spliced intervening intron of 221 nucleotides. To remove the intron, we amplified the two exons separately and ligated them. Exon 1 was amplified using a forward primer tailed with an *Hin*dIII (underlined) restriction site and a minimal T7 promoter (italic) (P1, 5′-CGAAGCTT*TAATACGACTCACTATA***GGG**CTGTGAA-3′, where a boldface G indicates positions that were mutated from T in the natural sequence to provide an efficient template for in vitro transcription) and a reverse primer tailed with a 20-nucleotide sequence from exon 2 that includes a natural *Acc*I site (underlined) (P2, 5′-CAGTCTACTTCCTCTGTGATGTTGTATTTTAAG-3′). Exon 2 was amplified using forward primer P3 (5′-AAGGCGCCATCACAGAGGAAGTAGACTGATAT-3′) and *Nco*I (underlined) tailed-reverse primer P4 (5′-TTCCATGGCCTTCCCAGAGGAAAAGC-3′). The amplified products were gel purified and separately subcloned in the pCR4Blunt-TOPO vector using a Zero Blunt PCR Cloning Kit (Invitrogen). After digestion and gel purification, the two exons were ligated using T4 DNA ligase (New England Biolabs), and the resulting product was PCR amplified using primers P1 and P4 and subcloned in pCR4Blunt-TOPO (pUTR). The *Firefly* luciferase gene was amplified from the pGL3 basic vector (Promega) using a forward primer tailed with *Nco*I (underlined) (P5, 5′-AACCATGGAAGACGCCAAAAACATAAAG-3′) and an *Acc*651 (underlined) tailed-reverse primer (P6, 5′-TTGGTACCTTACACGGCGATCTTTCCG-3′). In a three-piece ligation, the digested and gel-purified products from pUTR and the luciferase gene ligated at the *Nco*I site inserted into a *Hin*dIII- and *Acc*651-digested linear pUC18 vector (Promega). Positive clones were confirmed by DNA sequencing.

The plasmid encoding the control transcript *del-UTR* was obtained by deleting the 25-nucleotide G-quadruplex-forming sequence using the Quickchange site-directed mutagenesis kit (Stratagene). The deletion was conducted in two steps. The first 11 nucleotides of the G-quadruplex-forming sequence were deleted using forward primer P9 (5′-CTTCTTTCTCTGGTGGGAGCTGGGGCGAGAG-3′) and reverse primer P10 (5′-CCTCGCCCCAGCTCCCACCACAGAAAGAAG-3′). The next 14 nucleotides were removed using forward primer P11

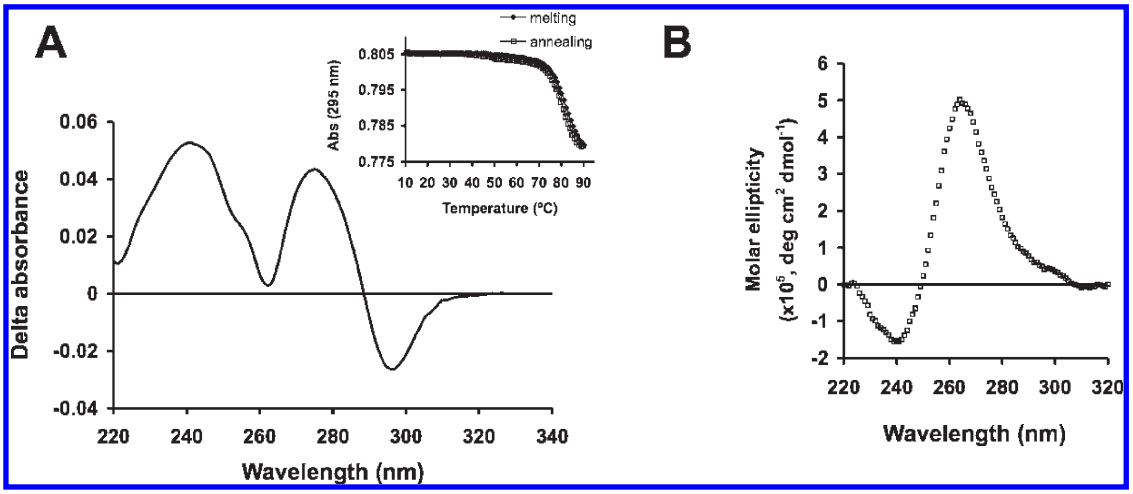

FIGURE 2: Biophysical analysis of the BCL2Q RNA G-quadruplex. (A) Thermal difference spectrum of the BCL2Q RNA G-quadruplex. The inset shows the thermal melting and annealing UV profiles. (B) CD spectrum of BCL2Q. Experiments were performed in 10 mM sodium cacodylate (pH 7.0) and 50 mM KCl.

(5′-CTCCTCTTCTTTCTCTCGAGAGGTGCCGTTGGCC-3′) and reverse primer P12 (5′-GGCCAACGGCACCTCTCGAGA-GAAAGAAGAGGAG-3′). The plasmids were sequenced to confirm the presence of the intended changes.

For cell-based experiements, the constructs were transferred into CMV promoter-driven mammalian expression vectors. An *Xba*I restriction site (underlined) was introduced using site-directed mutagenesis at the 3′ end of the *Firefly* luciferase coding sequence in the plasmids described above, using forward primer P13 (5′-GGGCGGAAAGATCGCCGTGTAATACCGAGC-TCTAGAATTCGTAATCATGG-3′) and reverse primer P14 (5′-CCATGATTACGAATTCTAGAGCTCGGTATTACAC-GGCGATCTTTCCGCCC-3′). The constructs were then cloned into the pRL-CMV vector (Promega) using *Hin*dIII and *Xba*I sites. The quadruplex-mutated plasmid (pCMV mut-UTR) was constructed by site-directed mutagenesis with forward primer P15 (5′-CTCTGGGGGCCGTTTTTTGGGAGCTGGGGCGAGA-GG-3′) and reverse primer P16 (5′-CCTCTCGCCCCAGCTCC-CAAAAAACGGCCCCCAGAG-3′).

In Vitro Transcription, in Vitro Translation, and Luciferase Assays. The plasmids were linearized at the 3′ end of the *Firefly* luciferase coding region using *Acc*651. The 5′ capped transcripts were synthesized in vitro using the mMessage mMachine T7 kit (Ambion) as previously described (*32*, *35*). RNA concentrations were determined by UV spectroscopy using a Nano Drop spectrophotometer. In vitro translation and luciferase assays were performed as previously described (*35*).

Cell Culture. Cells were grown to a confluency of 60−70% in flat bottom 24-well plates at 37 °C in a humidified atmosphere containing 5% CO_2. The medium for MCF10A cells was Dulbecco's Modified Eagle's Medium: Nutrient Mixture F-12 (DMEM/F12, Invitrogen), 5% horse serum, 2 mg of epidermal growth factor/100 mL, 50 μg of hydrocortisone/100 mL, 1 μg of cholera toxin/100 mL, and 10 μg of insulin/100 mL. HGC27 cells were grown in Eagle's Minimum Essential Medium (EMEM, Sigma), 2 mM L-glutamine, and 10% fetal bovine serum. MCF-7 cells were cultured in Dulbecco's Modified Eagle's Medium (DMEM, Sigma) supplemented with 10% fetal bovine serum.

Dual Luciferase and Quantitative RT-PCR Assays. Cells were cotransfected with 500 ng of *Firefly* reporter construct plasmid DNA and 50 ng of normalizing plasmid DNA pRL-TK (Promega) using TransIT-LT1 transfection reagent (Mirus) following the manufacturer's protocol. Twenty-four hours after transfection, *Renilla* and *Firefly* luciferase activities were measured using the Dual-Luciferase Reporter Assay system (Promega), following the manufacturer's protocol, on an Orion II microplate luminometer (Berthold). Total RNA was isolated using the RNeasy mini kit (Qiagen) according to the manufacturer's protocol. The RNA concentration was determined by UV spectroscopy, and 500 ng of total RNA was used in a 20 μL cDNA synthesis reaction using oligo(dT) primer (Invitrogen) and SuperScript III reverse trancriptase (Invitrogen) according to the manufacturer's protocol. For quantification of mRNA levels, 1 μL of the cDNA was used in a 10 μL reaction mixture with LightCycler 480 SYBR Green I Master (Roche) on a Roche LightCycler 480 instrument using the forward 5′-TGAGTACTTCGAAATGTCCGTTC-3′ and reverse 5′-GT-ATTCCAGCCCATATCGTTTCAT-3′ primers for *Firefly* and the forward 5′-CAGCATTTTCTGCATGTTTTTCTGAATC-3′ and reverse 5′-CTATAAGAACCATTACCAGATTTGC-3′ primers for *Renilla*. All the reactions were conducted in duplicate. The relative gene expression was calculated using an adequate mathematical model (*42*) [ratio = $(E_{\text{target}})^{\Delta CP_{\text{target}}(\text{control}-\text{sample})}/(E_{\text{reference}})^{\Delta CP_{\text{ref}}(\text{control}-\text{sample})}$] with *Firefly* as the target gene transcript in comparison to *Renilla* as the reference gene transcript. The mean values and their associated experimental errors were calculated from at least three independent experiments.

RESULTS

The BCL2Q Sequence Folds into a Thermodynamically Stable RNA G-Quadruplex. To determine whether the BCL2Q sequence folds into a G-quadruplex, we performed a series of biophysical experiments on a synthetic RNA oligonucleotide using UV and CD spectroscopic analysis. Qualitative structural information about the folded state of an oligonucleotide can be readily obtained by recording a thermal difference spectrum (*41*). The thermal difference spectrum obtained for BCL2Q exhibits a shape that is similar to that reported for G-quadruplex structures (Figure 2A), with two positive peaks at ~243 and ~273 nm and a negative peak at ~295 nm (*41*). Accordingly, the thermal melting profile of BCL2Q recorded at 295 nm in a sodium cacodylate buffer (pH 7.0) containing 50 mM KCl shows a characteristic hypochromic sigmoidal transition (Figure 2A, inset) (*43*), with a T_m values of 81 °C. Curves for

Table 2: T_m Values (degrees Celsius) of the BCL2Q RNA G-Quadruplex in the Presence of Various Monovalent Cations[a]

concentration (mM)	K^+	Na^+	Li^+
1	59	54	56
10	71	58	53
20	75	59	53
50	81	61	53

[a] T_m values are an average of three independent experiments and have an associated error of ±1 °C.

melting and annealing were superimposable, and studies over a 50-fold oligonucleotide concentration range (from 1 to 50 μM) showed no change (data not shown), which is consistent with intramolecular quadruplex formation. At a higher KCl concentration (100 mM), the structure could not be unfolded, even at 95 °C, indicating a very stable G-quadruplex under near-physiological salt conditions. The BCL2Q RNA G-quadruplex was fairly stable (T_m = 55 °C) even in the absence of any added stabilizing cations. An important charcteristic of G-quadruplex structures, as compared to those involving Watson−Crick base pairs, is their monovalent cation dependence for stabilization (*44*). In the presence of various monovalent cations, the stability of BCL2Q, as judged by T_m, showed the expected trend for G-quadruplex structure: $K^+ > Na^+ > Li^+$ (Table 2). CD spectrocopy can be used as a standard technique to analyze G-quadruplex conformation (*45*). At pH 7.0 and 50 mM KCl, the CD spectrum of BCl2Q exhibited a positive peak at 265 nm and a negative peak at 240 nm (Figure 2B), which is the typical CD signature of a parallel G-quadruplex structure (*45*).

The BCL2Q Motif Modulates the BCL-2 5′ UTR Translation Efficiency in Vitro. To specifically determine the influence of the BCL2Q motif on translation within its native context, we cloned the 493-nucleotide *BCL-2* 5′ UTR (Figure 1B) from human genomic DNA and inserted it immediately downstream of the minimal T7 promoter and upstream of the *Firefly* luciferase coding sequence in a plasmid expression vector. The *BCL-2* 5′ UTR that was examined in this study corresponds to transcript ENST00000333681 in the Ensembl database from which the alternatively spliced 221-nucleotide intron (Figure 1A) was excluded. It contains the 25-nucleotide BCL2Q motif located 426 nucleotides downstream from the 5′ end and 42 nucleotides upstream from the translation start site. In addition to the plasmid encoding the transcript that includes the wild-type *BCL-2* 5′ UTR (*wt-UTR*), we also generated a control plasmid in which the 25-nucleotide BCL2Q quadruplex-forming sequence has been deleted from the *BCL-2* 5′ UTR (transcript *del-UTR*). Corresponding transcripts were produced with a 5′ cap by in vitro transcription using T7 polymerase and subjected to in vitro translation using nuclease-treated rabbit reticulocyte lysate, which is an established eukaryotic cell-free system for studying translation (*46*). Translation efficiencies were measured by the standard luminescence assay for luciferase catalytic activity (*47*). The translation efficiency of an mRNA in reticulocyte lysates is sensitive to the amount of mRNA that is added to the reaction mixture (*46*, *48*). This is particularly true for those mRNAs that exhibit stable secondary structures in their 5′ UTR. We thus performed in vitro translation experiments using mRNA concentrations ranging from 10 to 320 ng/μL. As shown in Figure 3, for RNA concentrations of ≤20 ng/μL, we did not observe any differences in translation efficiency between the *del-UTR* and *wt-UTR* transcripts, indicating that the BCL2Q motif is not affecting in vitro translation. However,

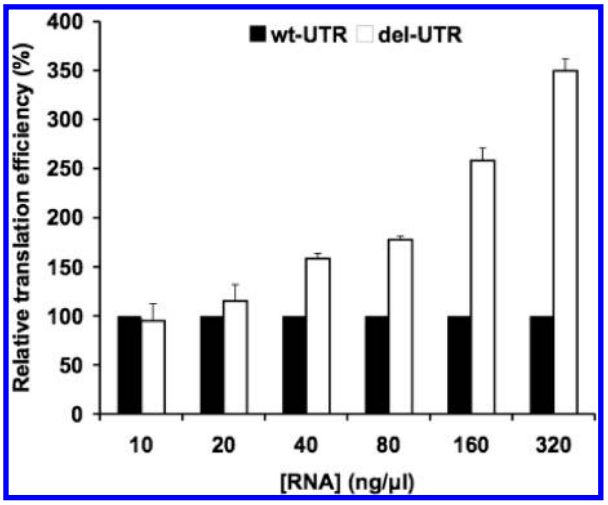

FIGURE 3: Relative in vitro translation efficiency of the wild-type *BCL2* 5′ UTR (*wt-UTR*) and the quadruplex-deleted 5′ UTR (*del-UTR*) at increasing mRNA concentrations, as judged by quantitation of *Firefly* luciferase activity. Error bars represent the sem of three independent experiments.

at higher mRNA concentrations, deletion of the RNA G-quadruplex motif resulted in an increase in mRNA translation efficiency. At an mRNA concentration of 320 ng/μL, the *del-UTR* transcript was translated 3.5-fold more efficiently that the *wt-UTR* transcript, showing that the BCL2Q RNA G-quadruplex motif has potential to inhibit translation.

The BCL2Q Motif Modulates the Translation Efficiency of the BCL-2 5′ UTR in Human Cells. To further investigate the aptitude of the BCL2Q motif to affect translation, we next performed dual luciferase assays in cultured human cells. The wild-type and quadruplex-deleted *BCL-2* 5′ UTR *Firefly* luciferase reporter constructs, used for the in vitro study, were transferred downstream from a CMV promoter into a mammalian expression vector (Figure 4A). For these studies, we also prepared a quadruplex-mutated *BCL-2* 5′ UTR construct (pCMV mut-UTR) by substituting one G_4 tract of the BCL2Q RNA with U_4 to disrupt RNA G-quadruplex formation, while maintaining the natural length of the 5′ UTR (Figure 4A). Each of the three vector constructs (pCMV wt-UTR, pCMV del-UTR, and pCMV mut-UTR) was cotransfected into MCF10A human breast epithelial cells together with a pRL-TK normalizing vector, which encodes the *Renilla* luciferase. Following a 24 h growth period, cells were harvested for dual luciferase assays and for quantitative RT-PCR on total RNA to measure transcript levels. Levels of *Firefly* luciferase activity and *Firefly* luciferase mRNA were normalized to the corresponding values obtained for *Renilla* luciferase and compared. As shown in Figure 4B, both deletion and mutation of the BCL2Q G-quadruplex-forming sequence resulted in an increase in the level of protein synthesis, by 2.3- and 1.9-fold, respectively. In contrast, the mRNA levels, as determined by quantitative RT-PCR analysis using an adequate mathematical model (*42*), were not significantly affected (Figure 4B). Qualitatively comparable results were also obtained in two other cell lines: human breast adenocarcinoma cell line MCF7 and human gastric carcinoma cell line HGC27 (Table 3). The translational suppressive effect of the BCL2Q motif was however much less pronounced in HGC27 cells. Collectively, these data demonstrate that the BCL2Q RNA G-quadruplex motif in the *BCL2* 5′ UTR has an inhibitory effect on translation in human cells.

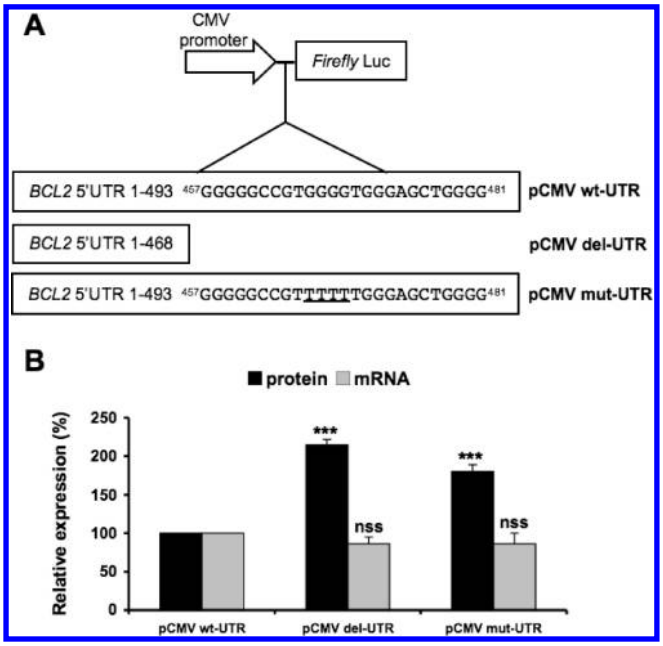

FIGURE 4: (A) Schematic representation of the DNA luciferase reporter constructs used in the study: pCMV wt-UTR, full-length (493 nucleotides) wild-type *BCL-2* 5′ UTR; pCMV del-UTR, from which the 25-nucleotide G-quadruplex-forming sequence has been deleted; and pCMV mut-UTR, full-length *BCL-2* 5′ UTR with a G_4-to-T_4 mutation (underlined) to disrupt G-quadruplex formation. (B) Relative protein levels, as judged by quantitation of luciferase activity, and mRNA levels, as judged by quantitative RT-PCR, from expression of the three constructs in MCF10A cultured cells. Results were normalized relative to the data obtained for the pCMV wt-UTR construct. Error bars represent the standard error of the mean of at least three independent experiments. Asterisks indicate $p < 0.001$; nss, not statistically significant (Student's *t* test).

Table 3: Relative *Firefly* Luciferase Protein and mRNA Expression of the Dual Luciferase (DL) Constructs in Different Cell Lines

	MCF7		HGC27	
construct	protein	mRNA	protein	mRNA
DL wt-UTR	100	100	100	100
DL del-UTR	230 ± 13^a	83 ± 13^b	139 ± 6^a	99 ± 17^b
DL mut-UTR	188 ± 14^a	121 ± 12^b	134 ± 6^a	113 ± 17^b

$^a p < 0.01$. ^{b}Not statistically significant (Student's *t* test).

DISCUSSION

Regulation of eukaryotic translation by G-rich sequences capable of folding into noncanonical four-stranded RNA G-quadruplex structures has recently emergerd as a new paradigm. In 2007, we reported the identification of a naturally occurring RNA G-quadruplex in the 5′ UTR of the human *NRAS* proto-oncogene and demonstrated its role in inhibiting translation in vitro (*32*). Subsequently, other RNA G-quadruplexes, found in the 5′ UTR of the human *ZIC-1* (*34*) and *MP3-MMP* (*36*) mRNAs, were shown to inhibit translation of reporter constructs in HeLa cells, and a G-quadruplex in the 5′ UTR of a *ERS1* mRNA variant was shown to repress translation in rabbit reticulocyte lysate (*38*). Halder et al. have also established general translation repression by artificially designed *cis*-acting 5′ UTR G-quadruplexes in several cell lines (*37*). While this work was under review, two reports have been published that used reporter-based constructs to describe posttranscriptional control of gene expression by RNA G-quadruplex-forming motifs in the 5′ UTRs of *TRF2*, in 293T cells (*49*), and six other genes, in HEK 293 cells (*50*). In a detailed computational analysis of the human transcriptome, we have identified ~2300 sequences with the potential to form RNA G-quadruplexes in the 5′ UTRs of genes (*40*). One such sequence (BCL2Q, 5′-GGGGGCCGUGGGGUGGGAGCUGGGG-3′) was found in the 5′ UTR of the *BCL-2* gene, which plays critical functions in controlling programmed cell death (*1*). The BCL2Q sequence is highly conserved in length, sequence, and position in the *BCL-2* 5′ UTR, across various species, including human, mouse, dog, horse, and dolphin (Table 1). In this work, we have investigated the ability of this sequence to form a stable structure and evaluated its effect on the translation efficiency of a *BCL-2* 5′ UTR.

The UV thermal difference spectrum, CD spectrum, and UV thermal melting experiments, performed in the presence of various monovalent cations, were all consistent with intramolecular RNA G-quadruplex formation by the BCL2Q sequence. In fact, the BCL2Q sequence folds into a thermodynamically very stable G-quadruplex, with a T_m of >80 °C in the presence of 50 mM KCl. At a near-physiological potassium concentration (100 mM), the BCL2Q RNA G-quadruplex could not be melted, even at 95 °C. Such extreme thermodynamic stability has also been observed for other naturally occurring 5′ UTR RNA G-quadruplexes (*32*, *34*, *36*, *38*) and is thought to result from the 2′-OH groups acting as a scaffold for a network of water molecules that lock the structure (*51*). The results from our biophysical study of the BCL2Q RNA G-quadruplex are also corroborated by a very recent report from Sugimoto and co-workers investigating the conformation and thermodymamics of a RNA G-quadruplex under crowding conditions using a mutant sequence (5′-AGGGC-CGUGGGGUGGGAGCUGGG-3′) derived from BCL2Q (*51*).

Next, we cloned the native full-length 493-nucleotide 5′ UTR of *BCL-2* upstream of the *Firefly* luciferase reporter gene, and immediately downstream of the minimal T7 promoter, to preserve the position of the G-quadruplex motif in the RNA 5′ UTR. It is noteworthy that this study represents one of the few examples [with the *NRAS* (*32*) *MT3-MMP* (*36*), and the very recent studies (*49*, *50*)] to investigate the influence of an RNA G-quadruplex on translation when it is located in its native context within the full-length wild-type 5′ UTR, a factor that we previously showed to be a determinant for translation repression by another naturally occurring RNA G-quadruplex-forming sequence in the *NRAS* 5′ UTR (*35*). We also prepared a control construct by deleting the 25-nucleotide BCL2Q quadruplex-forming sequence from the UTR. We then titrated the corresponding 5′ capped mRNAs, generated by in vitro transcription, in nuclease-treated rabbit reticulocyte lysate. When a low concentration of mRNA (≤20 ng/μL) was used, the luciferase expression of the RNA G-quadruplex-containing transcript (*wt-UTR*) was similar, within experimental error, to that of the control transcript (*del-UTR*). However, when the mRNA concentration was increased, a translational inhibitory effect of the RNA G-quadruplex structure was observed. The level of inhibition increased in a mRNA concentration-dependent manner from 40 to 320 ng/μL. It has been demonstrated that increasing the mRNA concentration in lysates, for mRNAs containing stable 5′ UTR secondary structures, enhances the demand for RNA helicase activity (e.g., from eIF4A and eIF4G) required for efficient scanning of the ribosomal translation initiation complex from the 5′ cap to the AUG translation start codon (*48*). Accordingly, under competitive conditions, at higher concentrations of input mRNA, the secondary structures can no longer be efficiently removed by the

limited amount of RNA helicase activity, resulting in translation inhibition (*48*). Our data show that at mRNA concentrations of >20 ng/μL, the *wt-UTR* transcript is increasingly less efficiently translated than the *del-UTR* transcript, indicating that the BCL2Q RNA G-quadruplex is inhibiting translation.

Having demonstrated that the BCL2Q motif has potential to inhibit translation in vitro, we then investigated whether it was still the case in cells. We performed dual luciferase assays in three types of human cell lines (MCF10A, MCF7, and HGC27) using CMV promoter-driven expression vectors that contain either wild-type (pCMV wt-UTR), quadruplex-deleted (pCMV del-UTR), or quadruplex-mutated (pCMV mut-UTR) *BCL-2* 5′ UTRs upstream of the *Firefly* luciferase coding sequence, and a normalizing vector that encodes the *Renilla* luciferase. Our data show that both deletion and mutation of the BCL2Q motif resulted in a significant increase in the level of *Firefly* luciferase expression, as compared to the wild-type *BCL-2* 5′ UTR, in all three cell lines. Using quantitative RT-PCR, we did not detect any significant difference in mRNA levels among the three constructs. We thus conclude that the increase in the level of *Firefly* expression occurs at the translational level rather than the transcriptional level, indicating that the BCL2Q RNA G-quadruplex-forming motif, in its native context, is inhibiting translation. A maximum inhibitory effect of 2.3-fold was obtained in MCF10A cells, whereas a 1.4-fold inhibition was observed in HGC27 cells. The reasons for this quantitative discrepancy between cell lines are not clear. Similar observations have been made using other RNA G-quadruplex-forming sequences and different eukaryotic cell lines (*37*). Cell-dependent variations in the level of translation repression may possibly be due to differences in the availability and/or efficiency of some components of the translation machinery (e.g., initiation factors or helicases) between cell lines.

Taken together, this work presents the first evidence of the existence and function of an RNA G-quadruplex motif in the 5′ UTR of *BCL-2* that inhibits translation. Overexpression of the anti-apoptotic Bcl-2 protein has been associated with neoplasia and chemotherapy resistance in various human cancers. Therefore, considerable effort is being directed toward small molecules that target Bcl-2 protein (*52*). Some of these molecules have demonstrate promising results in clinical trials, particularly in combination with other chemotherapy agents. Furthermore, one antisense oligonucleotide that targets the coding region of *BCL-2* mRNA and downregulates protein expression is currently in clinical trials (*52*, *53*). We have recently reported an in vitro proof of concept that an RNA G-quadruplex in the 5′ UTR can serve as a molecular target for G-quadruplex selective small molecule inhibition of translation (*54*). We will be exploring the potential of the BCL2Q RNA G-quadruplex as a target in future studies. Interestingly, a DNA G-quadruplex-forming sequence has also been identified upstream of the P1 promoter region of *BCL-2* (*55*−*57*). This could offer the possibility of inhibiting *BCL-2* expression at the transcriptional and translational levels via two independent G-quadruplex targets.

REFERENCES

1. Borner, C. (2003) The Bcl-2 protein family: Sensors and checkpoints for life-or-death decisions. *Mol. Immunol. 39*, 615–647.
2. Vaux, D. L., Cory, S., and Adams, J. M. (1988) Bcl-2 gene promotes haemopoietic cell survival and cooperates with c-myc to immortalize pre-B cells. *Nature 335*, 440–442.
3. Tsujimoto, Y., Cossman, J., Jaffe, E., and Croce, C. M. (1985) Involvement of the bcl-2 gene in human follicular lymphoma. *Science 228*, 1440–1443.
4. Tsujimoto, Y., Gorham, J., Cossman, J., Jaffe, E., and Croce, C. M. (1985) The t(14;18) chromosome translocations involved in B-cell neoplasms result from mistakes in VDJ joining. *Science 229*, 1390–1393.
5. Cleary, M. L., Smith, S. D., and Sklar, J. (1986) Cloning and structural analysis of cDNAs for bcl-2 and a hybrid bcl-2/immunoglobulin transcript resulting from the t(14;18) translocation. *Cell 47*, 19–28.
6. Graninger, W. B., Seto, M., Boutain, B., Goldman, P., and Korsmeyer, S. J. (1987) Expression of Bcl-2 and Bcl-2-Ig fusion transcripts in normal and neoplastic cells. *J. Clin. Invest. 80*, 1512–1515.
7. Desoize, B. (1994) Anticancer drug resistance and inhibition of apoptosis. *Anticancer Res. 14*, 2291–2294.
8. Schmitt, C. A., and Lowe, S. W. (2001) Bcl-2 mediates chemoresistance in matched pairs of primary E(mu)-myc lymphomas in vivo. *Blood Cells Mol. Dis. 27*, 206–216.
9. Reed, J. C., Meister, L., Tanaka, S., Cuddy, M., Yum, S., Geyer, C., and Pleasure, D. (1991) Differential expression of bcl2 protooncogene in neuroblastoma and other human tumor cell lines of neural origin. *Cancer Res. 51*, 6529–6538.
10. McDonnell, T. J., Troncoso, P., Brisbay, S. M., Logothetis, C., Chung, L. W., Hsieh, J. T., Tu, S. M., and Campbell, M. L. (1992) Expression of the protooncogene bcl-2 in the prostate and its association with emergence of androgen-independent prostate cancer. *Cancer Res. 52*, 6940–6944.
11. Pezzella, F., Turley, H., Kuzu, I., Tungekar, M. F., Dunnill, M. S., Pierce, C. B., Harris, A., Gatter, K. C., and Mason, D. Y. (1993) bcl-2 protein in non-small-cell lung carcinoma. *N. Engl. J. Med. 329*, 690–694.
12. Bronner, M. P., Culin, C., Reed, J. C., and Furth, E. E. (1995) The bcl-2 proto-oncogene and the gastrointestinal epithelial tumor progression model. *Am. J. Pathol. 146*, 20–26.
13. Reed, J. C., Miyashita, T., Krajewski, S., Takayama, S., Aime-Sempe, C., Kitada, S., Sato, T., Wang, H. G., Harigai, M., Hanada, M., Krajewska, M., Kochel, K., Millan, J., and Kobayashi, H. (1996) Bcl-2 family proteins and the regulation of programmed cell death in leukemia and lymphoma. *Cancer Treat. Res. 84*, 31–72.
14. Satou, T., Cummings, B. J., and Cotman, C. W. (1995) Immunoreactivity for Bcl-2 protein within neurons in the Alzheimer's disease brain increases with disease severity. *Brain Res. 697*, 35–43.
15. Bar-Am, O., Weinreb, O., Amit, T., and Youdim, M. B. (2005) Regulation of Bcl-2 family proteins, neurotrophic factors, and APP processing in the neurorescue activity of propargylamine. *FASEB J. 19*, 1899–1901.
16. Seto, M., Jaeger, U., Hockett, R. D., Graninger, W., Bennett, S., Goldman, P., and Korsmeyer, S. J. (1988) Alternative promoters and exons, somatic mutation and deregulation of the Bcl-2-Ig fusion gene in lymphoma. *EMBO J. 7*, 123–131.
17. Young, R. L., and Korsmeyer, S. J. (1993) A negative regulatory element in the bcl-2 5′-untranslated region inhibits expression from an upstream promoter. *Mol. Cell. Biol. 13*, 3686–3697.
18. Smith, M. D., Ensor, E. A., Coffin, R. S., Boxer, L. M., and Latchman, D. S. (1998) Bcl-2 transcription from the proximal P2 promoter is activated in neuronal cells by the Brn-3a POU family transcription factor. *J. Biol. Chem. 273*, 16715–16722.
19. Wu, Y., Mehew, J. W., Heckman, C. A., Arcinas, M., and Boxer, L. M. (2001) Negative regulation of bcl-2 expression by p53 in hematopoietic cells. *Oncogene 20*, 240–251.
20. Duan, H., Heckman, C. A., and Boxer, L. M. (2007) The immunoglobulin heavy-chain gene 3′ enhancers deregulate bcl-2 promoter usage in t(14;18) lymphoma cells. *Oncogene 26*, 2635–2641.
21. Bredow, S., Juri, D. E., Cardon, K., and Tesfaigzi, Y. (2007) Identification of a novel Bcl-2 promoter region that counteracts in a p53-dependent manner the inhibitory P2 region. *Gene 404*, 110–116.
22. Kondo, E., Nakamura, S., Onoue, H., Matsuo, Y., Yoshino, T., Aoki, H., Hayashi, K., Takahashi, K., Minowada, J., and Nomura, S.; et al. (1992) Detection of bcl-2 protein and bcl-2 messenger RNA in normal and neoplastic lymphoid tissues by immunohistochemistry and in situ hybridization. *Blood 80*, 2044–2051.
23. Chleq-Deschamps, C. M., LeBrun, D. P., Huie, P., Besnier, D. P., Warnke, R. A., Sibley, R. K., and Cleary, M. L. (1993) Topographical dissociation of BCL-2 messenger RNA and protein expression in human lymphoid tissues. *Blood 81*, 293–298.
24. Ravazoula, P., Tsamandas, A. C., Kardamakis, D., Gogos, C., Karatza, C., Thomopoulos, K., Tepetes, K., Kourelis, T., Petsas, T., Bonikos, D. S., and Karavias, D. (2002) The potential role of bcl-2 mRNA and protein expression in hepatocellular carcinomas. *Anticancer Res. 22*, 1799–1805.

25. Pesole, G., Mignone, F., Gissi, C., Grillo, G., Licciulli, F., and Liuni, S. (2001) Structural and functional features of eukaryotic mRNA untranslated regions. *Gene 276*, 73–81.
26. Negrini, M., Silini, E., Kozak, C., Tsujimoto, Y., and Croce, C. M. (1987) Molecular analysis of mbcl-2: Structure and expression of the murine gene homologous to the human gene involved in follicular lymphoma. *Cell 49*, 455–463.
27. Eguchi, Y., Ewert, D. L., and Tsujimoto, Y. (1992) Isolation and characterization of the chicken bcl-2 gene: Expression in a variety of tissues including lymphoid and neuronal organs in adult and embryo. *Nucleic Acids Res. 20*, 4187–4192.
28. Sato, T., Irie, S., Krajewski, S., and Reed, J. C. (1994) Cloning and sequencing of a cDNA encoding the rat Bcl-2 protein. *Gene 140*, 291–292.
29. Harigai, M., Miyashita, T., Hanada, M., and Reed, J. C. (1996) A cis-acting element in the BCL-2 gene controls expression through translational mechanisms. *Oncogene 12*, 1369–1374.
30. Sherrill, K. W., Byrd, M. P., Van Eden, M. E., and Lloyd, R. E. (2004) BCL-2 translation is mediated via internal ribosome entry during cell stress. *J. Biol. Chem. 279*, 29066–29074.
31. Bonnal, S., Schaeffer, C., Creancier, L., Clamens, S., Moine, H., Prats, A. C., and Vagner, S. (2003) A single internal ribosome entry site containing a G quartet RNA structure drives fibroblast growth factor 2 gene expression at four alternative translation initiation codons. *J. Biol. Chem. 278*, 39330–39336.
32. Kumari, S., Bugaut, A., Huppert, J. L., and Balasubramanian, S. (2007) An RNA G-quadruplex in the 5′ UTR of the NRAS proto-oncogene modulates translation. *Nat. Chem. Biol. 3*, 218–221.
33. Khateb, S., Weisman-Shomer, P., Hershco-Shani, I., Ludwig, A. L., and Fry, M. (2007) The tetraplex $(CGG)_n$ destabilizing proteins hnRNP A2 and CBF-A enhance the in vivo translation of fragile X premutation mRNA. *Nucleic Acids Res. 35*, 5775–5788.
34. Arora, A., Dutkiewicz, M., Scaria, V., Hariharan, M., Maiti, S., and Kurreck, J. (2008) Inhibition of translation in living eukaryotic cells by an RNA G-quadruplex motif. *RNA 14*, 1290–1296.
35. Kumari, S., Bugaut, A., and Balasubramanian, S. (2008) Position and stability are determining factors for translation repression by an RNA G-quadruplex-forming sequence within the 5′ UTR of the NRAS proto-oncogene. *Biochemistry 47*, 12664–12669.
36. Morris, M. J., and Basu, S. (2009) An unusually stable G-quadruplex within the 5′-UTR of the MT3 matrix metalloproteinase mRNA represses translation in eukaryotic cells. *Biochemistry 48*, 5313–5319.
37. Halder, K., Wieland, M., and Hartig, J. S. (2009) Predictable suppression of gene expression by 5′-UTR-based RNA quadruplexes. *Nucleic Acids Res. 37*, 6811–6817.
38. Balkwill, G. D., Derecka, K., Garner, T. P., Hodgman, C., Flint, A. P., and Searle, M. S. (2009) Repression of translation of human estrogen receptor α by G-quadruplex formation. *Biochemistry 48*, 11487–11495.
39. Neidle, S., and Balasubramanian, S. (2006) Quadruplex Nucleic Acids, RSC Biomolecular Sciences, Cambridge, U.K.
40. Huppert, J. L., Bugaut, A., Kumari, S., and Balasubramanian, S. (2008) G-Quadruplexes: The beginning and end of UTRs. *Nucleic Acids Res. 36*, 6260–6268.
41. Mergny, J. L., Li, J., Lacroix, L., Amrane, S., and Chaires, J. B. (2005) Thermal difference spectra: A specific signature for nucleic acid structures. *Nucleic Acids Res. 33*, e138.
42. Pfaffl, M. W. (2001) A new mathematical model for relative quantification in real-time RT-PCR. *Nucleic Acids Res. 29*, e45.
43. Mergny, J. L., Phan, A. T., and Lacroix, L. (1998) Following G-quartet formation by UV-spectroscopy. *FEBS Lett. 435*, 74–78.
44. Hardin, C. C., Watson, T., Corregan, M., and Bailey, C. (1992) Cation-dependent transition between the quadruplex and Watson-Crick hairpin forms of $d(CGCG_3GCG)$. *Biochemistry 31*, 833–841.
45. Paramasivan, S., Rujan, I., and Bolton, P. H. (2007) Circular dichroism of quadruplex DNAs: Applications to structure, cation effects and ligand binding. *Methods 43*, 324–331.
46. Merrick, W. C., and Barth-Baus, D. (2007) Use of reticulocyte lysates for mechanistic studies of eukaryotic translation initiation. *Methods Enzymol. 429*, 1–21.
47. DiLella, A. G., Hope, D. A., Chen, H., Trumbauer, M., Schwartz, R. J., and Smith, R. G. (1988) Utility of firefly luciferase as a reporter gene for promoter activity in transgenic mice. *Nucleic Acids Res. 16*, 4159.
48. Gallie, D. R. (2007) Use of in vitro translation extract depleted in specific initiation factors for the investigation of translational regulation. *Methods Enzymol. 429*, 35–51.
49. Gomez, D., Guédin, A., Mergny J. L., Salles, B., Riou, J. F., Teulade-Fichou, M. P., Calsou P. (2010) A G-quadruplex structure within the 5′-UTR of TRF2 mRNA represses translation in human cells, *Nucleic Acids Res*. Advance Access published on June 22, 2010 doi:10.1093/nar/gkq563.
50. Beaudoin, J. D., and Perreault, J. P. (2010) 5′-UTR G-quadruplex structures acting as translational repressors. *Nucleic Acids Res*. doi: 10.1093/nar/gkq557.
51. Zhang, D. H., Fujimoto, T., Saxena, S., Yu, H. Q., Miyoshi, D., and Sugimoto, N. (2010) Monomorphic RNA G-quadruplex and polymorphic DNA G-quadruplex structures responding to cellular environmental factors. *Biochemistry 49*, 4554–4563.
52. Kang, M. H., and Reynolds, C. P. (2009) Bcl-2 inhibitors: Targeting mitochondrial apoptotic pathways in cancer therapy. *Clin. Cancer Res. 15*, 1126–1132.
53. Dias, N., and Stein, C. A. (2002) Potential roles of antisense oligonucleotides in cancer therapy. The example of Bcl-2 antisense oligonucleotides. *Eur. J. Pharm. Biopharm. 54*, 263–269.
54. Bugaut, A., Rodriguez, R., Kumari, S., Hsu, S. T., and Balasubramanian, S. (2010) Small molecule-mediated inhibition of translation by targeting a native RNA G-quadruplex. *Org. Biomol. Chem. 8*, 2771–2776.
55. Dai, J., Chen, D., Jones, R. A., Hurley, L. H., and Yang, D. (2006) NMR solution structure of the major G-quadruplex structure formed in the human BCL2 promoter region. *Nucleic Acids Res. 34*, 5133–5144.
56. Dexheimer, T. S., Sun, D., and Hurley, L. H. (2006) Deconvoluting the structural and drug-recognition complexity of the G-quadruplex-forming region upstream of the bcl-2 P1 promoter. *J. Am. Chem. Soc. 128*, 5404–5415.
57. Dai, J., Dexheimer, T. S., Chen, D., Carver, M., Ambrus, A., Jones, R. A., and Yang, D. (2006) An intramolecular G-quadruplex structure with mixed parallel/antiparallel G-strands formed in the human BCL-2 promoter region in solution. *J. Am. Chem. Soc. 128*, 1096–1098.